EGTRIB Journal
JOURNAL OF
THE EGYPTIAN SOCIETY OF TRIBOLOGY
VOLUME 21, No. 2, April 2024, pp. 105 – 119 **ISSN 2090 - 5882**
(Received October 23. 2023, Accepted in final form February 26. 2024) **jest.journals.ekb.eg**

OPTIMIZING MRI-BASED MEDICAL DIAGNOSIS: COMPARATIVE ANALYSIS OF EFFICIENTNET PERFORMANCE WITH VARYING LEARNING RATES

Wael Abouelwafa Ahmed[1], Mohamed A. Massoud[1] and Mohamed E. El-Bouridy[2]

[1]Department of Biomedical Engineering, Faculty of Engineering, Minia University, Minia, 61519, EGYPT.
[2]Alexandria Higher Institute of Engineering &Technology, Alex., EGYPT.

ABSTRACT

Magnetic Resonance Imaging (MRI) has emerged as a fundamental tool in the field of medical diagnostics, offering detailed insights into anatomical structures. As the demand for efficient and accurate diagnosis increases, leveraging deep learning techniques becomes imperative, among which the learning rate stands out as a pivotal factor influencing model convergence and generalization. In this research, we investigate the influence of varying learning rates on the efficacy of the EfficientNet B0 model, a cutting-edge convolutional neural network design acclaimed for its efficiency and proficiency in tasks related to image classification. Our comparative analysis unveils the profound influence of learning rates on the diagnostic accuracy and efficiency of the model. Specifically, we observe that optimal learning rates significantly enhance the convergence speed and overall performance of EfficientNet in medical image.

In conclusion, this research highlighting the importance of learning rates in improving diagnostic precision and efficacy. We observed a wide range of outcomes in terms of training and validation accuracy, as well as training and validation losses. Notably, Trial 1 and Trial 2, which utilized lower initial learning rates (0.001 and 0.01, respectively), achieved higher validation accuracy compared to Trial 3, where the initial learning rate was set to 0.1. This suggests that tuning learning rates may lead to better convergence and generalization in the training process

KEYWORDS

MRI, EfficientNet, classification models, learning rates, medical diagnosis.

INTRODUCTION

Magnetic Resonance Imaging (MRI) has become prominent as an indispensable tool for visualizing internal anatomical structures and detecting pathological abnormalities with unparalleled precision, This imaging modality provides enhanced differentiation of soft tissues and the ability to visualize anatomy from multiple perspectives, rendering it particularly advantageous for the diagnosis of a broad range of medical conditions, spanning neurological disorders, musculoskeletal injuries, and oncological malignancies, [1].

In recent decades, the progression of MRI technology has been marked by significant advancements, characterized by enhancements in magnetic field strengths, expedited imaging sequences, and innovative contrast agents. These developments have catalyzed the transformation of diagnostic imaging to unparalleled levels of sophistication, extending from routine screening examinations to intricate interventional procedures, MRI has significantly transformed clinical methodologies across diverse medical disciplines, equipping healthcare practitioners with indispensable understandings of the fundamental pathophysiological mechanisms of diseases, [2]. Concurrent with the expansive growth of MRI medical imaging datasets, the emergence of deep learning methodologies signifies a transformative epoch in the realm of medical image interpretation, presenting unprecedented prospects for automated disease identification, delineation, and categorization. Notably, convolutional neural networks (CNNs), among other deep learning architectures, have exhibited exceptional efficacy in discerning hierarchical patterns from medical imagery, achieving superior diagnostic accuracy beyond human capabilities across various clinical assessments, [3].

The application of machine learning in the field of biological sciences has showed considerable efficacy, as machine learning methodologies exhibit superior descriptive capabilities compared to traditional biomedical models. Beyond offering engineering solutions, these techniques also facilitate nuanced insights, thereby contributing to advanced comprehension within the field.[4, 5].
An exemplary application of machine learning is its role in the identification of brain tumors. Although a definitive universal cure for cancer remains elusive, early cancer detection holds promise for mitigating mortality rates. Tumors are categorized as either benign or malignant. Benign tumors, being noncancerous, do not metastasize, Thus, it lacks the ability to propagate throughout the body. Malignant tumors, on the other hand, are malignant and can infiltrate adjacent tissues before spreading throughout the body to form secondary tumors, [6, 7].

Positron emission tomography (PET) and magnetic resonance imaging (MRI) are the imaging modalities available for obtaining critical data about brain malignancies.
MRI stands out as a widely employed technique due to its inherent benefits. Utilizing both 2D and 3D formats, MRI yields pertinent insights into the morphology, spatial orientation, dimensions, and histological characteristics of brain lesions. The implementation of computer-aided diagnosis (CAD) systems offers a promising avenue for automating tumor detection, thereby alleviating the laborious and time-intensive task of manual image review, [8 - 11].

The diverse array of inter- and intra-structural shapes, contrast variations, and textures depicted in MRI images pose a formidable challenge to address, [12, 13]. Employing conventional machine learning (ML) methodologies for classification entails the manual extraction of features. Conversely, CNN models possess the capability to automatically extract pertinent features, thereby enhancing performance substantially. However, gathering a large volume of data for training a deep learning-based model remains a daunting task, [14, 15]. However, because to the contrast differences and diverse form textures, it remains a struggle.

Rao et al., [16], conducted pixel-wise classifications through the acquisition of deep representations for individual pixels, incorporating information from multiple modalities including T1, T1c, T2, and Flair. Subsequently, these representations were combined to provide a complete multimodal representation of each pixel. The categorization was subsequently carried out using a CNN model, with an accuracy rate of 67%, according to Afshar et al., [17].

Saxena et al. attained an accuracy of 86.56% through the implementation of a singular CNN layer featuring 64 attribute maps, coupled with 16 primary type capsules, [18]. It was suggested that pre-trained models, specifically Vgg16, InceptionV3, and ResNet50, be used for the purpose. Among these transfer learning techniques, ResNet50 produced the greatest accuracy of 95%. Furthermore, in the realm of CNN-LSTM architectures, Shahzadi et al. demonstrated an 84% accuracy peak utilizing VggNet-LSTM, [19, 20]. El Abbadi et al., [21], obtained 96.66% accuracy in categorization using Singular Value Decomposition (SVD). However, they employed a dataset with just 20 normal and 50 aberrant data points. Mohsen et al., [22]. The current study supports the use of discrete wavelet transform (DWT) as a robust feature extraction strategy alongside principal component analysis (PCA) in a Deep Neural Network (DNN) classification architecture. This new technique gives an impressive accuracy of 93.94%. Çinar & Yildirim, [10]. The authors propose using an improved model to identify brain cancers. This upgraded model was created by using ResNet-50 as a foundational model, then omitting the final five levels and including ten additional layers, increasing the layer count from 177 to 182. The additional layers were added in the following order: Relu, Batch Normalization, Dropout, Fully connected, Relu, Max pooling, Fully connected, Classification, and Softmax. With this combination, they achieved a high accuracy of 97.01%.

In the domain of medical image analysis, EfficientNet has demonstrated considerable efficacy across various tasks including lesion detection, organ segmentation, and disease classification, highlighting its capacity to enhance clinical decision-making and ultimately enhance patient outcomes. Leveraging the innate hierarchical organization inherent in medical images, EfficientNet possesses the capability to detect nuanced patterns and deviations that might evade human observation, thereby presenting a compelling opportunity for advancing diagnostic precision and streamlining efficiency, [23 - 26].

Moreover, the selection of learning rate scheduling methods, encompassing fixed rates, annealing schedules, and adaptive techniques, adds complexity to the optimization process, requiring thorough experimentation and refinement to attain peak performance. Fluctuations in learning rates wield a significant impact on the course of model training, affecting aspects such as convergence velocity, robustness, and generalization capacity. Hence, meticulous attention is imperative in devising and executing deep learning frameworks for medical image analysis, [27 - 33].

This study attempts to address the following research objectives:

- **To evaluate the efficacy of EfficientNet B0 in the classification of MRI images for medical diagnosis.**
- **Analyze how different learning rates affect EfficientNet B0 convergence and classification accuracy.**

- **Examine how learning rate optimization affects model performance in MRI-based medical diagnostics.**

Based on the stated research objectives, our hypotheses are as follows: Variations in learning rates will significantly impact the convergence behavior and classification accuracy of EfficientNet B0.

Section two of the present paper provides an in-depth review of a full description of the dataset utilized, the architecture of the model employed, and the experimental design used for our analysis. Moving on to Section 3, the findings of the present trials will be discussed. Here, we exhaustively describe EfficientNetB0's performance data across several learning rates. This investigation aims to give insights into the usefulness of various learning rate settings and their impact on the model's performance in medical image analysis tasks.

In section 4, the consequences of our findings will be discussed. The relevance of learning rate optimization in the context of MRI-based medical diagnosis will discussed. By critically assessing the consequences of our study findings, we want to contribute to a more comprehensive knowledge of deep learning model performance in medical imaging applications.

Finally, section 5 concludes the present paper. Here, the important findings from the study and identify prospective areas for further research will be summarized. The future developments in the field of medical image processing by summarizing our work's overall contributions and recommending topics for further investigation will be stimulated.

The goal of this extensive research is not only increase our understanding of deep learning model performance in medical image analysis but also build the framework for the creation of more accurate and efficient diagnostic tools in clinical practice.

METHODOLOGY

MRI Dataset Selection and Preprocessing

Dataset Description:

The MRI dataset used in this study is divided into four classes: glioma tumors, pituitary tumors, meningiomas, and pituitary tumor, [34]. The training dataset has 2670 photos, whereas the validation dataset contains 394 images, as shown in Table 1 and Fig. 1.

Preprocessing Techniques:

After importing the original dataset and before model training, the MRI images were preprocessed to guarantee consistency and quality. Data augmentation to enhance the number of images was employed. By enriching the dataset, the classification model performance improves. The photos were downsized to fit the network input layer (224 224 3), followed by the intensity and spatial normalization to a standardized template. All preprocessing processes were accomplished using [MATLAB tools], [35].

Efficient Net B0 Architecture and Model Configuration

Efficient Net Overview:

A CNN architecture known as EfficientNet, [36], presented the leverages compound coefficients for effective scaling.

Efficient Net presents a pioneering methodology in neural network architecture, employing compound scaling to systematically adapt model depth, width, and resolution for optimal performance within computational limitations. This innovative approach guarantees state-of-the-art accuracy across a spectrum of resource constraints, thereby demonstrating remarkable versatility in deployment across diverse scenarios.

Table 1. Dataset summary

	Glioma Tumor	Meningioma Tumor	Pituitary Tumor	Pituitary Tumor
Training data set	826	822	827	395
Testing dataset	100	115	74	105

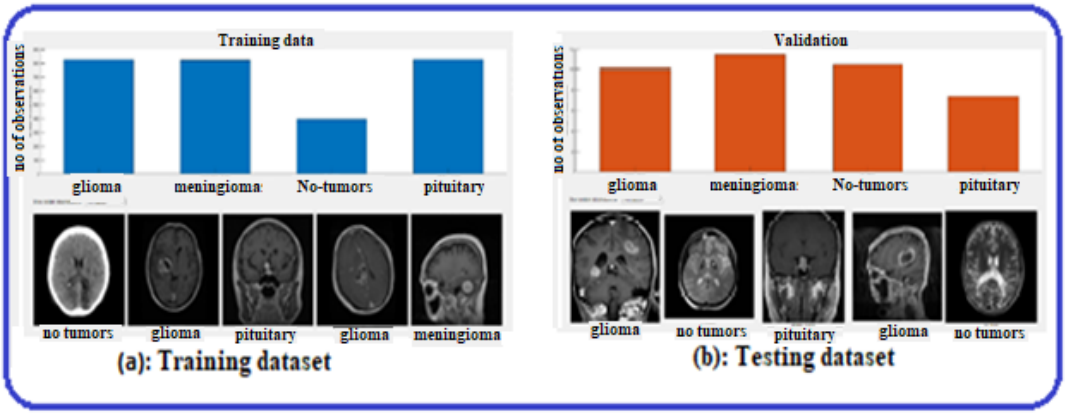

Fig. 1. The training, and testing datasets.

The lowest Trainable Parameters about five millions leads to lower computational time than other models, as shown in Table 2. EfficientNet is fundamentally structured around a hierarchical framework, incorporating various foundational components such as convolutional layers, normalization layers, and activation functions. These constituents are meticulously coordinated to optimize feature extraction efficiency while mitigating computational burdens. Prominent architectural components encompass depth wise separable convolutions, squeeze-and-excitation blocks, and streamlined attention mechanisms, collectively underpinning the model's outstanding efficacy in image classification endeavors.

The concept of model scaling, which aims to increase performance by increasing network depth, breadth, and resolution, was presented in the EfficientNet article for Image Classification. Fig. *2* shows the architecture of EfficientNet with the influence of different models. Recognizing the success of the method exhibited by EfficientNet, researchers expanded it to Object Detection, culminating in the invention of EfficientDet. In the early stages of EfficientNet, the authors created a basic network architecture called Efficient Net, which was created using Neural Architecture Search (NAS). Building on this foundation, a team at Google suggested a unique method of architecture development utilizing NAS in combination with Reinforcement Learning, resulting in the design of an

Efficient Net variation optimized for both accuracy and compute efficiency, as measured by FLOPS.

1) Increasing Depth: Deeper structures frequently performed better because they could collect more complicated and changeable data, making them more adaptable to new applications. However, training deeper networks offers substantial challenges, primarily because of the vanishing gradient problem. Despite concerted efforts to alleviate this issue with techniques such as batch normalization and residual connections.

2) Expanding Width: Increased channel count in convolution layers is a typical strategy in compact models. This method has been widely used in previous efforts, such as MobileNets and MNasNet. Broader networks may capture complex features and are often more trainable. Nonetheless, networks that are extremely broad yet shallow may struggle to understand higher-level properties, resulting in a plateau in accuracy improvement when the networks get too large.

3) Enhancing Resolution: Utilizing input images of higher resolutions enables Convolutional Neural Networks (ConvNets) to potentially capture more intricate patterns. While earlier iterations of ConvNets typically employed input resolutions of 224x224, contemporary architectures favor resolutions of 299x299 or 331x331 to bolster precision. Recent strides in the field, exemplified by GPipe, have demonstrated cutting-edge accuracy on ImageNet datasets, achieving resolutions as expansive as 480x480. Moreover, ConvNets designed for object detection often integrate even larger resolutions, such as 600x600.

4) compound Scaling: Achieving optimal accuracy and efficiency in ConvNets necessitates balancing network width, depth, and resolution comprehensively. Compound Scaling, which involves synergistically adjusting all dimensions of network architecture, emerges as a crucial strategy in ConvNet scaling. This holistic approach ensures that improvements in accuracy are accompanied by enhanced computational efficiency.

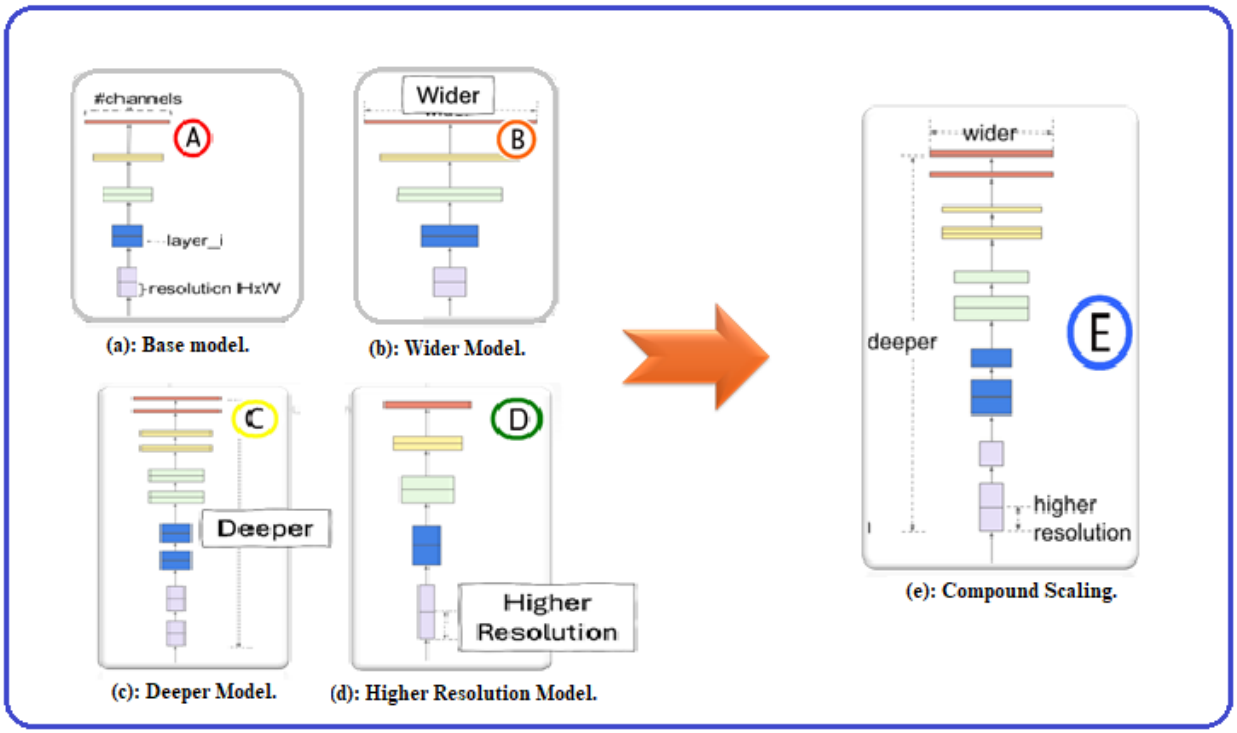

Fig. 2.The architecture of EfficientNet with different models.

By exploring the individual effects of scaling depth, width, and resolution, we arrive at the understanding that while scaling any dimension can enhance accuracy, the magnitude of accuracy gain diminishes for larger models. This insight lays the groundwork for investigating methodologies like neural Architecture Search, as exemplified in the development of EfficientNet by the authors.

1.1. Scaling Efficient-B0 to get B1-B7

Scaling Up ConvNets are commonly utilized for improved accuracy. ResNet [36] may be scaled up from ResNet-18 to ResNet-1000 [27] by employing more layers. ResNet-1000 has similar accuracy as ResNet-101 although having many more layers.

This section explains the EffcientNet Architecture. Let the network number of layers (N), layer width(W) and input image size (S) be:

$$\text{number of layers: } N = \alpha^{\phi} \quad (1)$$

$$\text{layer width: } W = \beta^{\phi} \quad (2)$$

$$\text{Image size: } S = \gamma^{\phi} \quad (3)$$

$$\text{s.t.} \quad \alpha \cdot \beta^2 \cdot \gamma^2 \approx 2 \quad (4)$$

$$\alpha \geq 1, \beta \geq 1, \gamma \geq 1 \quad (5)$$

φ, a user-defined coefficient, defines the amount of extra resources available.

The variables α, β, and γ define the distribution of additional resources among networks based on their depth (d), width (w), and input resolution.

If we have extra resources, we may use a small grid search to identify α, β, and γ. This allows us to scale the depth, width, and input resolution of the network to increase its size.

Starting from the baseline EfficientNet-B0, Apply a compound scaling method to scale it up with two steps:

STEP 1: Set φ = 1, assuming twice as many resources, and do a tiny grid search for α, β, and γ. The optimal parameters for EfficientNet-B0 are α = 1.2, β = 1.1, and γ = 1.15, with a constraint of α * β2 * γ2 ≈ 2.

STEP 2: Fix α, β, and γ as constants and scale up the baseline network with varying φ to achieve EfficientNet-B1 to B7.

Estimating a number of parameters and layers for EfficientNet B10, B9, and B8 based on the typical patterns observed in the EfficientNet series as shown in Table *2* The estimates were derived from the scaling factors applied to the base EfficientNet architecture. As the models in the EfficientNet series increase in scale, they tend to follow a consistent pattern of growth in terms of parameters and layers. These estimates are based on extrapolation from the known properties of the earlier models in the series.

Table 2. hyper parameters specification for Efficient Net B0 to predicted B10

Model	Trainable Parameters	total number of layers	Computational Cost
EfficientNet-B0	Around 5 million	Around 215	Low
EfficientNet-B1	Around 7 million	Around 230	Low to Moderate
EfficientNet-B2	Around 9 million	Around 245	Moderate
EfficientNet-B3	Around 12 million	Around 260	Moderate
EfficientNet-B4	Around 20 million	Around 275	Moderate to High
EfficientNet-B5	Around 30 million	Around 290	High
EfficientNet-B6	Around 43 million	Around 305	High
EfficientNet-B7	Around 66 million	Around 320	High
EfficientNet-B8	Around 87 million	Around 335	High
EfficientNet-B9	Around 130 million	Around 350	High

EfficientNet-B10	Around 180 million	Around 365	Very High

1.2. EfficientNet B0 Model Configuration:

In this work, we used the EfficientNet B0 variation as the core architecture for our classification model. EfficientNet B0 maintains a healthy balance between model complexity and computational economy, making it a great candidate for applications demanding high classification accuracy within resource-constrained situations.

The configuration of EfficientNet B0 adopted in our experiments is as follows:

- **Input Dimensions: The model ingests input images of dimensions [224 224 3], ensuring compatibility with the preprocessed MRI images in our dataset.**
- **Architecture Overview: EfficientNet B0 is characterized by a series of stacked blocks, each comprising a sequence of convolutional layers, activation functions, and normalization layers. These blocks are meticulously designed to capture hierarchical features within the input images, enabling the model to discern subtle anatomical and pathological patterns in MRI scans. Fig. 3 illustrates the stacked blocks diagram of EfficientNet B0.**
- **Parameterization: The model parameters, including the number of convolutional filters, kernel sizes, and strides, are meticulously calibrated to optimize performance while minimizing computational overhead. This ensures that the model achieves a favorable trade-off between accuracy and efficiency, facilitating seamless integration into real-world applications.**
- **Output Layer: The final layer of the network consists of a dense layer followed by a softmax activation function, enabling multi-class (four classes) classification of MRI images into distinct diagnostic categories.**

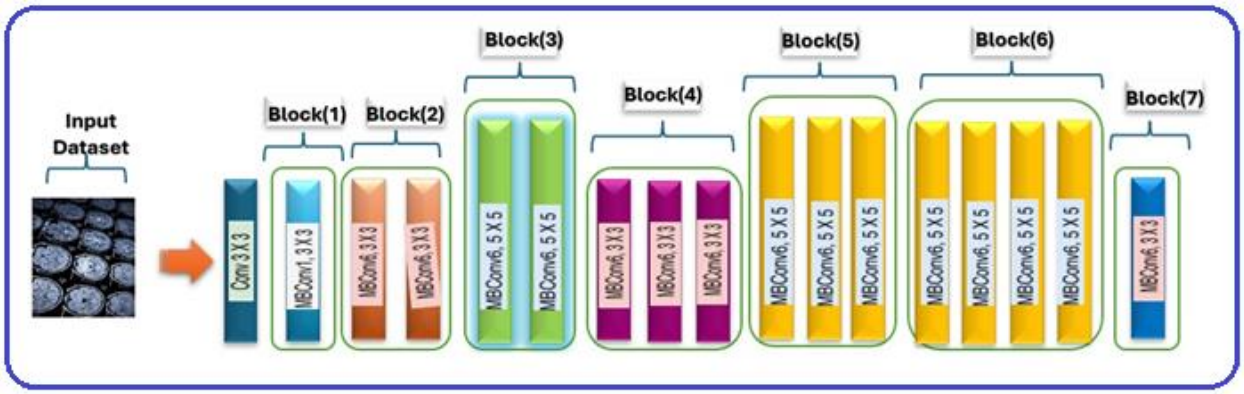

Fig. 3.EfficientNet B0 Blocks structure

1.3. Experimental Setup

Using the MRI image collection, three sets of tests were conducted to detect brain tumors. In each collection, EfficientNet B0 was used to classify the existence of tumors with varying learning rates.

1) Training Protocol: The classification model was trained using a [Lenovo Z50 with Intel(R) Core(TM) i7-4510U CPU @ 2.00GHz 2.60 GHz, 16.0 GB RAM and NVIDIA GPU GeForce 840M, 4GB memory, DirectX 11]

To study the influence of learning rates on model convergence and performance, we used a systematic technique of adjusting learning rates throughout numerous trials. We investigated a variety of learning rates, including [0.001,0.01, and 0.1], and used dynamic learning rate scheduling strategies (exponential decay).*Evaluation Metrics*

1) Performance Metrics: A confusion matrix was used to evaluate model performance, which included accuracy, precision, recall, and F1-score. These metrics give extensive

insights into the classification model's ability to effectively differentiate between the four tumor classifications.

2) Cross-Validation: To reduce the danger of overfitting and check model generalization, we used cross-validation. Ensure an equitable distribution of participants throughout training, validation, and test sets.

2. Results:

2.1. Summary of Experiment Trials with Varying Efficient Net B0 Model and Learning Rates :

In this series of experiments, we investigated the impact of changing the learning rate on the performance of the EfficientNet B0 model. The trials were conducted on a single GPU, with each experiment varying the learning rate while keeping other hyperparameters constant. which yield valuable insights into model performance and training dynamics. From the results obtained, it is evident that the choice of learning rate plays a crucial role in determining the convergence and generalization of the models. Table 3 shows the experiment summary of three trials.

Trial 1 and Trial 2, where lower initial learning rates (0.001 and 0.01, respectively) were employed, exhibited higher validation accuracy compared to Trial 3, which utilized a higher initial learning rate (0.1). This suggests that lower learning rates may facilitate better convergence and enable the models to generalize well to unseen data.

Furthermore, it is noteworthy that while Trial 3 achieved a relatively lower training accuracy, it did not translate to comparable performance on the validation set, indicating potential overfitting or poor generalization. This emphasizes the importance of carefully tuning hyperparameters, including learning rates, to strike a balance between model complexity and generalization. Fig. *4* -Fig. 6 show Accuracy, loss of training, confusion matrix of training, and validation data at the three trials (0.001 and 0.01, 0.1) as mentioned before

Table 3. summary of three trial experiments

Experiential Details			Hyperparameters	Metrics			
Trial	Execution	Elapsed Time H:Min: sec	Learning Rate	Training Accuracy (%)	Training Loss	Validation Accuracy (%)	Validation Loss
1	Single GPU	4: 43: 23	0.0010	100	0.12	78.93	0.85
2	Single GPU	4: 36:16	0.0100	100	0.07	80.46	1.15
3	Single GPU	4:31:31	0.1000	72.7	0.86	71.07	1.22

Fig. 4-a. Training Plot (trial-1 at learning rate =0.001)

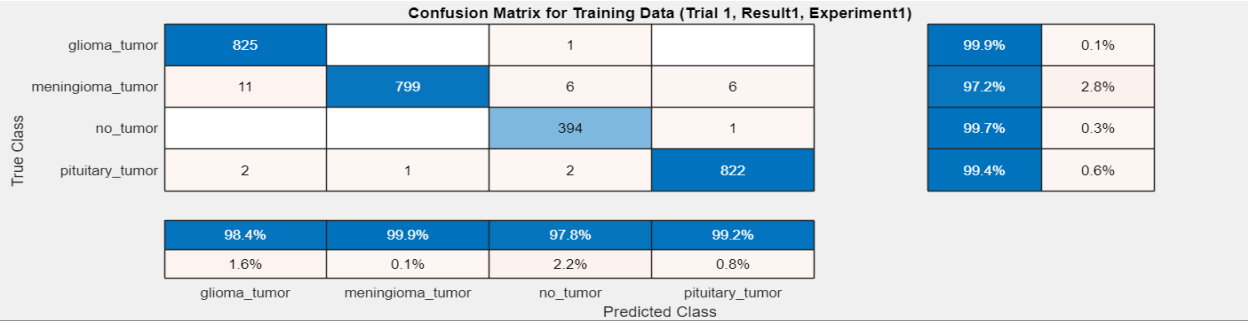

Fig.4-b. confusion matrix for training data (trial-1 at learning rate =0.001)

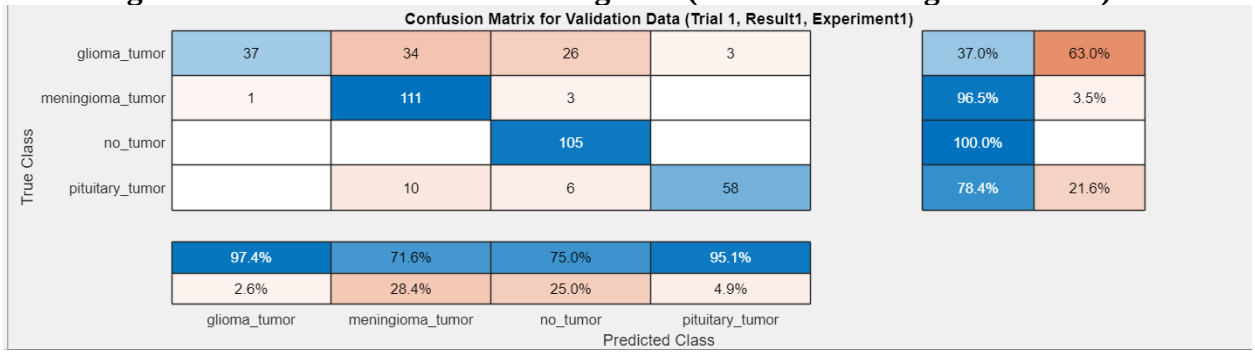

Fig.4-c. confusion matrix for validation data (trial-1 at learning rate =0.001)

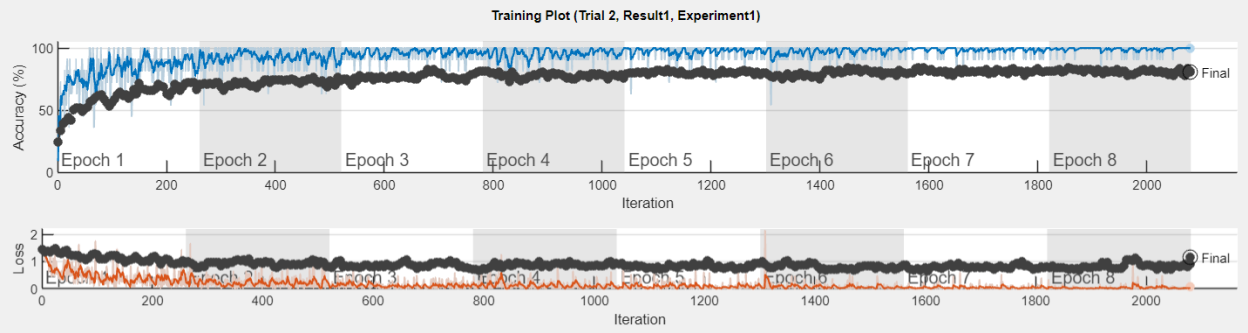

Fig. 5-a. Training Plot (trial-2 at learning rate =0.01)

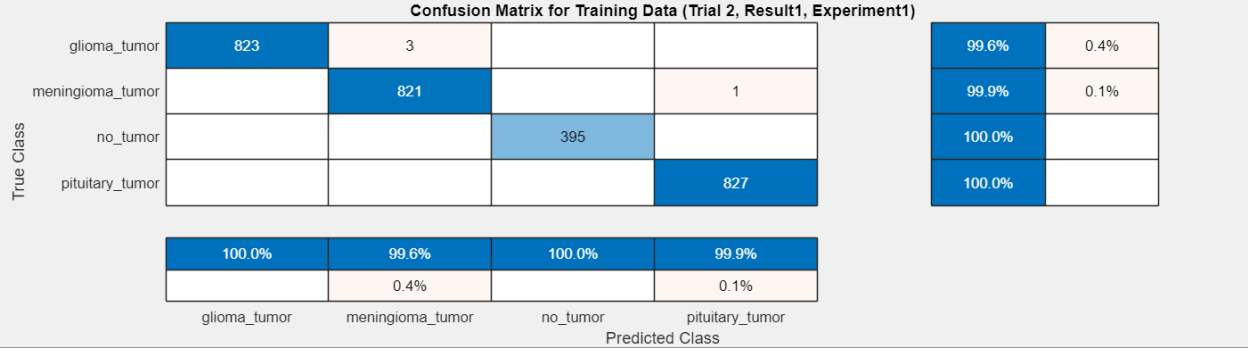

Fig. 5-b. confusion matrix for training data (trial-2 at learning rate =0.01)

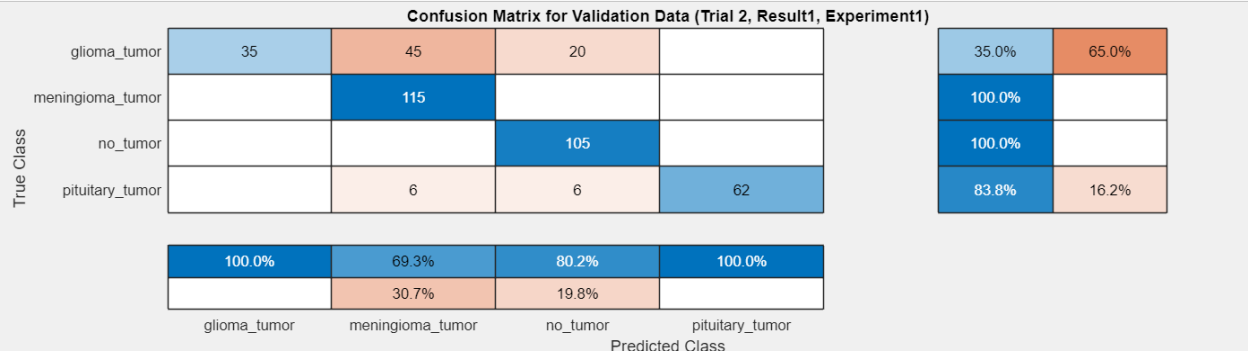

Fig. 5-c. confusion matrix for validation data (trial-2 at learning rate =0.01)

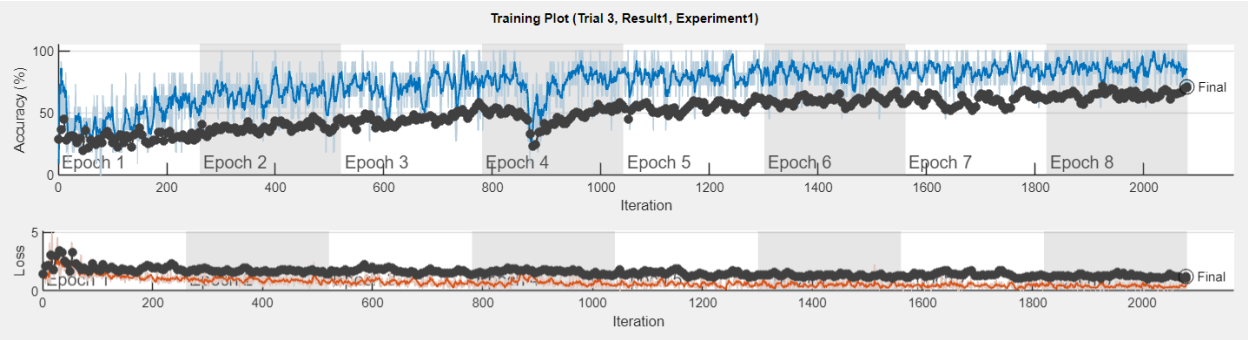

Fig. 6-a. Training Plot (trial-3 at learning rate =0.1)

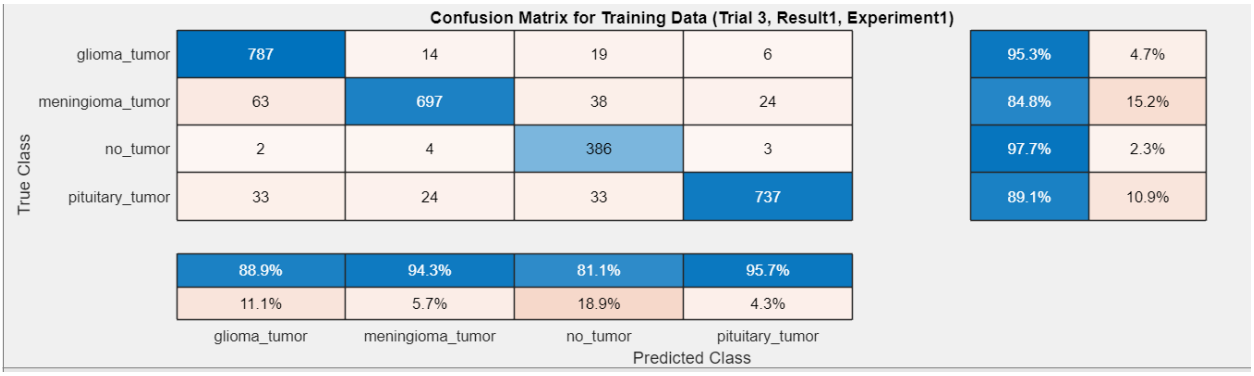

Fig. 6-b. confusion matrix for training data (trial-3 at learning rate =0.1)

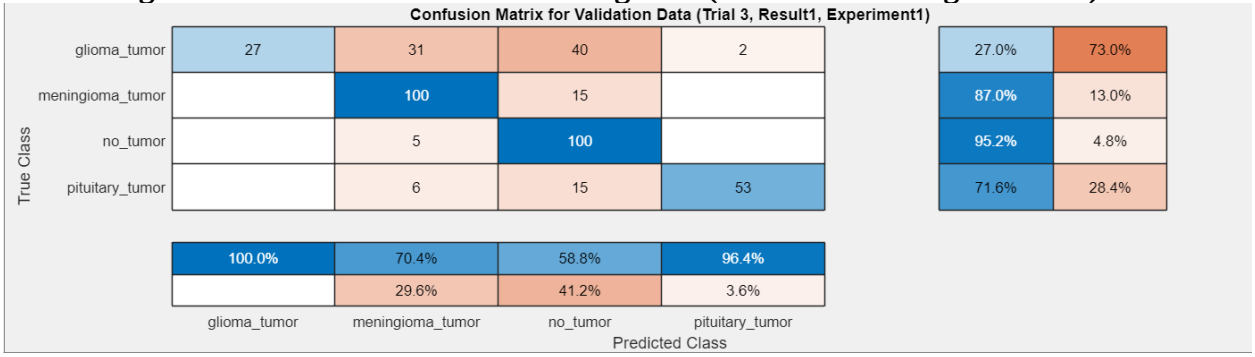

Fig. 6-c. confusion matrix for validation data (trial-3 at learning rate =0.1)

3. Discussion:

The observed differences in model performance across the trials underscore the intricate interplay between learning rates and model convergence. While lower learning rates tend to foster better convergence and generalization, excessively low learning rates may prolong training time and hinder the model's ability to adapt to the data effectively. Higher learning rates, on the other hand, may result in faster convergence but also increase the danger of overshooting the ideal solution or experiencing instability during training.

It is crucial to note that the optimal learning rate may vary depending on factors such as dataset characteristics, model architecture, and task complexity. Therefore, a systematic approach to hyperparameter tuning, possibly through techniques like grid search or random search, is essential to identify the most suitable learning rate for a given task.

Moreover, future research could explore dynamic learning rate scheduling strategies, such as learning rate decay or cyclical learning rates, to adaptively adjust the learning rate during training based on the model's performance. Additionally, ensembling models trained with different learning rates could potentially yield further improvements in accuracy and robustness.

Overall, these findings contribute to our understanding of the role of learning rates in training deep learning models and provide valuable insights for optimizing model performance in real-world applications.

Across the trials, we observed varying performance in terms of training and validation accuracy, as well as training and validation loss. Notably, Trial 1 and Trial 2, which utilized lower initial learning rates (0.001 and 0.01, respectively), achieved higher validation accuracy compared to Trial 3, where the initial learning rate was set to 0.1. This suggests that lower learning rates may lead to better convergence and generalization in the training process. A resulting conclusion in our experiments illustrates that a 0.01 learning rate gave the same accuracy as a lower learning rate (0.001) but with less computational time consumed when we tried to increase the learning rate to (0.1) to converge faster the model as shown is getting worse accuracy and precision .

4. Conclusion:

In summary, this research underscores the critical role of learning rates in the training of deep learning models, particularly in the context of medical image diagnosis using Magnetic Resonance Imaging (MRI) scans. By investigating the impact of varying learning rates on the performance of the EfficientNet B0 model, we have clarified critical thoughts into optimizing diagnostic precision and efficiency.

Our findings reveal a delicate balance between learning rates and model convergence, where lower learning rates tend to facilitate better convergence and generalization. However, excessively low learning rates may prolong training time without substantial

gains, while higher learning rates risk overshooting optimal solutions or encountering instability.

The experiments highlight that a learning rate of 0.01 achieves comparable accuracy to the lower rate of 0.001 but with reduced computational time. Conversely, increasing the learning rate to 0.1 results in diminished accuracy and precision, indicating the importance of selecting an appropriate learning rate to balance convergence speed and performance.

These observations emphasize the need for a systematic approach to hyperparameter tuning, considering factors such as dataset characteristics, model architecture, and task complexity. Future research avenues could explore dynamic learning rate scheduling strategies and ensemble techniques to further enhance model robustness and accuracy.

Overall, this study contributes to advancing our understanding of learning rate optimization in deep learning and provides valuable guidance for optimizing model performance in medical image diagnosis and other real-world applications.

5. FUTURE WORK

Conduct more research on various big batch optimizers for EfficientNet 1-7, such as the SM3 optimizer, to increase accuracy at high batch sizes.

Furthermore, model parallelism is a future topic of research that would enhance present data parallelism by allowing training on huge numbers of devices without conventional global batch sizes.

REFERENCES

1. B. Nunna Jr, P. Parihar, M. Wanjari, N. Shetty, and N. Bora, "High-Resolution Imaging Insights into Shoulder Joint Pain: A Comprehensive Review of Ultrasound and Magnetic Resonance Imaging (MRI)," *Cureus*, vol. 15, no. 11, pp. e48974–e48974, doi: 10.7759/cureus.48974, (Nov. 2023).

2. H. Kabasawa, "MR Imaging in the 21st Century: Technical Innovation over the First Two Decades," *Magnetic resonance in medical sciences : MRMS : an official journal of Japan Society of Magnetic Resonance in Medicine*, vol. 21, no. 1, pp. 71–82, doi: 10.2463/mrms.rev.2021-0011, (Mar. 2022).

3. H.-P. Chan, R. K. Samala, L. M. Hadjiiski, and C. Zhou, "Deep Learning in Medical Image Analysis," *Advances in experimental medicine and biology*, vol. 1213, pp. 3–21, doi: 10.1007/978-3-030-33128-3_1, (2020).

4. S. Tripathy and T. Swarnkar, "Unified Preprocessing and Enhancement Technique for Mammogram Images," *Procedia Computer Science*, vol. 167, pp. 285–292, doi: 10.1016/j.procs.2020.03.223, (2020).

5. V. Rao, M. S. Sarabi, and A. Jaiswal, "Brain tumor segmentation with deep learning," *MICCAI multimodal brain tumor segmentation challenge (BraTS)*, vol. 59, pp. 1–4, (2015).

6. S. Tripathy and T. Swarnkar, "Performance observation of mammograms using an improved dynamic window based adaptive median filter," *Journal of Discrete Mathematical Sciences and Cryptography*, vol. 23, no. 1, pp. 167–175, doi: 10.1080/09720529.2020.1721881, (2020).

7. P. Saxena, A. Maheshwari, and S. Maheshwari, "Predictive Modeling of Brain Tumor: A Deep Learning Approach," *Advances in Intelligent Systems and Computing*. Springer Singapore, pp. 275–285, doi: 10.1007/978-981-15-6067-5_30, (2020).

8. S. Tripathy and T. Swarnkar, "Investigation of the FFANN model for mammogram classification using an improved gray level co-occurrences matrix," *Int. J. Adv. Sci. Technol*, vol. 29, no. 4, pp. 4214–4226, (2020).

9. P. Rastogi, K. Khanna, and V. Singh, "LeuFeatx: Deep learning–based feature extractor for the diagnosis of acute leukemia from microscopic images of peripheral blood smear," *Computers in Biology and Medicine*, vol. 142, p. 105236, 2022, doi: 10.1016/j.compbiomed.105236,(2020).
10. A. Çinar and M. Yildirim, "Detection of tumors on brain MRI images using the hybrid convolutional neural network architecture," *Medical Hypotheses*, vol. 139, p. 109684, 2020, doi: 10.1016/j.mehy109684. (2020).
11. S. Tripathy and R. Singh, "Convolutional Neural Network: An Overview and Application in Image Classification," *Advances in Intelligent Systems and Computing*. Springer Nature Singapore, pp. 145–153, doi: 10.1007/978-981-16-4538-9_15, (2022).
12. S. Akcay, M. E. Kundegorski, M. Devereux, and T. P. Breckon, "Transfer learning using convolutional neural networks for object classification within X-ray baggage security imagery," *2016 IEEE International Conference on Image Processing (ICIP)*. IEEE, doi: 10.1109/icip.2016.7532519, (2016).
13. S. Christodoulidis, M. Anthimopoulos, L. Ebner, A. Christe, and S. Mougiakakou, "Multisource Transfer Learning With Convolutional Neural Networks for Lung Pattern Analysis," *IEEE Journal of Biomedical and Health Informatics*, vol. 21, no. 1, pp. 76–84, doi: 10.1109/jbhi.2016.2636929, (2017).
14. O. Sevli, "Performance Comparison of Different Pre-Trained Deep Learning Models in Classifying Brain MRI Images," *Acta Infologica*, vol. 5, no. 1, pp. 141–154, doi: 10.26650/acin.880918, (2021).
15. A. ARI and D. HANBAY, "Deep learning based brain tumor classification and detection system," *TURKISH JOURNAL OF ELECTRICAL ENGINEERING & COMPUTER SCIENCES*, vol. 26, no. 5, pp. 2275–2286, doi: 10.3906/elk-1801-8, (2018).
16. P. Gokila Brindha, M. Kavinraj, P. Manivasakam, and P. Prasanth, "Brain tumor detection from MRI images using deep learning techniques," *IOP Conference Series: Materials Science and Engineering*, vol. 1055, no. 1, p. 12115, doi: 10.1088/1757-899x/1055/1/012115, (2021).
17. S. Albawi, T. A. Mohammed, and S. Al-Zawi, "Understanding of a convolutional neural network," *2017 International Conference on Engineering and Technology (ICET)*. IEEE, 2017, doi: 10.1109/icengtechnol, 8308186, (2017).
18. M. K. Abd-Ellah, A. I. Awad, A. A. M. Khalaf, and H. F. A. Hamed, "A review on brain tumor diagnosis from MRI images: Practical implications, key achievements, and lessons learned," *Magnetic Resonance Imaging*, vol. 61, pp. 300–318, doi: 10.1016/j.mri.2019.05.028, (2019).
19. M. Alotaibi and B. Alotaibi, "Detection of COVID-19 Using Deep Learning on X-Ray Images," *Intelligent Automation & Soft Computing*, vol. 29, no. 3, pp. 885–898, doi: 10.32604/iasc.2021.018350, (2021).
20. X. Yin, D. Wu, Y. Shang, B. Jiang, and H. Song, "Using an EfficientNet-LSTM for the recognition of single Cow's motion behaviours in a complicated environment," *Computers and Electronics in Agriculture*, vol. 177, p. 105707, 2020, doi: 10.1016/j.compag,105707, (2020).
21. A. Işın, C. Direkoğlu, and M. Şah, "Review of MRI-based Brain Tumor Image Segmentation Using Deep Learning Methods," *Procedia Computer Science*, vol. 102, pp. 317–324, doi: 10.1016/j.procs.2016.09.407, (2016).
22. H. Mohsen, E.-S. A. El-Dahshan, E.-S. M. El-Horbaty, and A.-B. M. Salem, "Classification using deep learning neural networks for brain tumors," *Future Computing and Informatics Journal*, vol. 3, no. 1, pp. 68–71, doi: 10.1016/j.fcij.2017.12.001, (2018).

23. M. Tan and Q. Le, "Efficientnet: Rethinking model scaling for convolutional neural networks," in *International conference on machine learning*, PMLR, pp. 6105–6114, (2019).
24. S. Zhu *et al.*, "Screening of Common Retinal Diseases Using Six-Category Models Based on EfficientNet," *Frontiers in medicine*, vol. 9, p. 808402, doi: 10.3389/fmed.2022.808402, (Feb. 2022).
25. B. Pang, "Classification of images using EfficientNet CNN model with convolutional block attention module (CBAM) and spatial group-wise enhance module (SGE)," *International Conference on Image, Signal Processing, and Pattern Recognition (ISPP 2022)*. SPIE, doi: 10.1117/12.2636811, (2022).
26. J. Shao, H. Wu, and H. Liu, "Fine-grained recognition based on improved EfficientNet model," *2021 IEEE International Conference on Unmanned Systems (ICUS)*. IEEE, doi: 10.1109/icus52573.2021.9641257, (2021).
27. L. L. Xie, Y. Gong, K. R. Dong, C. Shen, B. Duan, and R. Dong, "Application of Machine Learning and Deep EfficientNets in Distinguishing Neonatal Adrenal Hematomas From Neuroblastoma in Enhanced Computed Tomography Images," *World journal of oncology*, vol. 15, no. 1, pp. 81–89, doi: 10.14740/wjon1744, (Feb. 2024).
28. Y. Dai, J. Li, Y. Ying, B. Zhang, T. Shi, and H. Zhao, "A Lightweight Fault Diagnosis Model of Rolling Bearing Based on Gramian Angular Field and EfficientNet-B0," *Lecture Notes of the Institute for Computer Sciences, Social Informatics and Telecommunications Engineering*. Springer Nature Switzerland, pp. 188–199doi: 10.1007/978-3-031-53404-1_16, (2024).
29. B. Zheng *et al.*, "Research on an artificial intelligence-based myopic maculopathy grading method using EfficientNet," *Indian journal of ophthalmology*, vol. 72, no. Suppl 1, pp. S53–S59, doi: 10.4103/IJO.IJO_48_23, (Jan. 2024).
30. A. Batool and Y.-C. Byun, "Lightweight EfficientNetB3 Model Based on Depthwise Separable Convolutions for Enhancing Classification of Leukemia White Blood Cell Images," *IEEE Access*, vol. 11, pp. 37203–37215, doi: 10.1109/access.2023.3266511, , (2023).
31. A. Hussain, S. Ul Amin, M. Fayaz, and S. Seo, "An Efficient and Robust Hand Gesture Recognition System of Sign Language Employing Finetuned Inception-V3 and Efficientnet-B0 Network," *Computer Systems Science and Engineering*, vol. 46, no. 3, pp. 3509–3525, doi: 10.32604/csse.2023.037258, (2023).
32. K. Ramamurthy, A. R. Varikuti, B. Gupta, and N. Aswani, "A deep learning network for Gleason grading of prostate biopsies using EfficientNet," *Biomedical Engineering / Biomedizinische Technik*, vol. 68, no. 2, pp. 187–198, doi: 10.1515/bmt-2022-0201, (2022).
33. F. Zulfiqar, U. Ijaz Bajwa, and Y. Mehmood, "Multi-class classification of brain tumor types from MR images using EfficientNets," *Biomedical Signal Processing and Control*, vol. 84, p. 104777, doi: 10.1016/j.bspc.2023.104777, (2023).
34. S. Bhuvaji, A. Kadam, P. Bhumkar, S. Dedge, and S. Kanchan, "Brain Tumor Classification (MRI)," *URL https://www. kaggle. com/dsv/1183165*, (2020).
35. "Appendix A: History of MATLAB and The MathWorks, Inc.," *Basic MATLAB®, Simulink®, and Stateflow®*. American Institute of Aeronautics and Astronautics, pp. 425–428. doi: 10.2514/5.9781600861628.0425.0428, (2007).
36. K. He, X. Zhang, S. Ren, and J. Sun, "Deep Residual Learning for Image Recognition," in *2016 IEEE Conference on Computer Vision and Pattern Recognition (CVPR)*, IEEE, pp. 770–778. doi: 10.1109/CVPR.2016.90, (Jun. 2016).